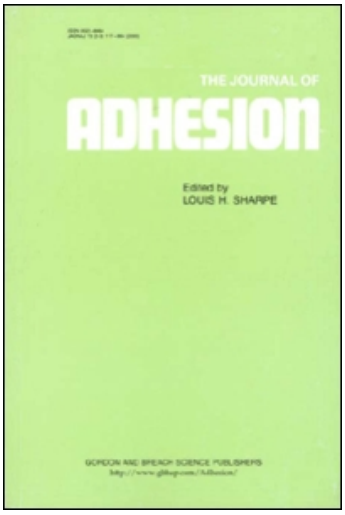

The Journal of Adhesion

Publication details, including instructions for authors and subscription information:
http://www.informaworld.com/smpp/title~content=t713453635

The Fracture Toughness of Adhesive-Bonded Joints

Wabtan A. Jemian[a]; Marie B. Ventrice[ab]
[a] Department of Mechanical Engineering, Auburn University, Auburn, Alabama [b] Mechanical Engineering Department, Tennessee Tech. University, Cookeville, Tenn.

Online publication date: 05 November 2010

To cite this Article Jemian, Wabtan A. and Ventrice, Marie B.(1969) 'The Fracture Toughness of Adhesive-Bonded Joints', The Journal of Adhesion, 1: 3, 190 — 207
To link to this Article: DOI: 10.1080/00218466908078892
URL: http://dx.doi.org/10.1080/00218466908078892

The Fracture Toughness of Adhesive-Bonded Joints

WARTAN A. JEMIAN AND MARIE B. VENTRICE*

Department of Mechanical Engineering
Auburn University
Auburn, Alabama 36830

(Received May 20, 1969)

ABSTRACT

Fracture mechanics is related to adhesion theory and the testing of adhesive-bonded joints in the lap-shear configuration. The complexity of the stress field necessitates the strain energy release rate approach, which is followed to derive the relation for a lap-shear sample: $G_c = P_c^2/4b\ (dC/da)$. G_c is the fracture toughness (critical strain energy release rate), P_c is the breaking or crack instability load, a and b are crack lengths and widths, respectively, and C is the sample compliance for the lap-shear sample with a crack of these dimensions at each loading edge. It was found that G_c ranged from 1.18 to 1.42 with an average value of 1.34 in.-lb./in.^{2} for epoxy bonded aluminum strips (EPON 934 and Alcald 2024-T3). Evidence, in the form of photoelastic stress patterns, suggesting that crack extension occurs in the opening mode in lap-shear samples is presented and discussed.

I. INTRODUCTION

FRACTURE MECHANICS is the study of the strength of a structural member that contains a crack; it provides a measure of the resistance to rapid crack growth. A normally ductile member may behave in a brittle manner if it contains cracks or other flaws. Adhesive-bonded joints are prone to flaws within the joint due to the complexity of shape, chemical dissimilarities, and assembly procedures. These flaws are frequently concentrated at the interfaces and under load may develop into cracks with a resulting brittle failure.

The study of brittle fracture has developed into the science of fracture mechanics which provides a method to calculate the magnitude of load that may be supported by a crack-containing member if the size of the possible cracks is known [1-4]. Or, if the expected load is known the size of the tolerable cracks may be calculated.

* Present address. Mechanical Engineering Department, Tennessee Tech. University, Cookeville, Tenn., 38501.

A variety of applications for fracture mechanics may be anticipated. Adhesives are frequently used to fasten the high strength sheet materials in which brittle fracture is a problem; design often includes the use of the adhesive-bonded joint as a barrier to further crack propagation; and although adhesives are especially prone to the development of flaws, they are normally tested using samples that are carefully prepared to ensure the absence of flaws. Each of these situations calls for special considerations with respect to crack extension.

The relationship of fracture toughness to adhesion is direct. Adhesion is here taken as a structure-sensitive mechanical property of a composite system in which chemical bonding has already been established. Adhesion has been measured in many ways, as is discussed by Gardon [5], and is represented by many parameters in a variety of dimensions. It is most significant that adhesive failure involves separation of the test piece by the growth or spreading of a crack. Even though the mechanism of crack growth precludes a direct measurement of adhesive bond strength by means of simultaneous, elastic separation of the two surfaces, the magnitude of this adhesive bond strength is an important part of the criterion for crack extension.

Fracture mechanics involves different parameters and a different point-of-view than the mechanics of homogeneous materials. Its application to composite systems in adhesion studies may shed more light on the distinction between adhesive and cohesive failures.

Only recently, have attempts been made to extend the concept to adhesive-bonded joints [6-9]. This work used two special types of joint configuration (see Fig. 1). Neither is typical of those used in engineering applications but each allows the study of crack extension, through the adhesive or along the interface, under carefully controlled conditions.

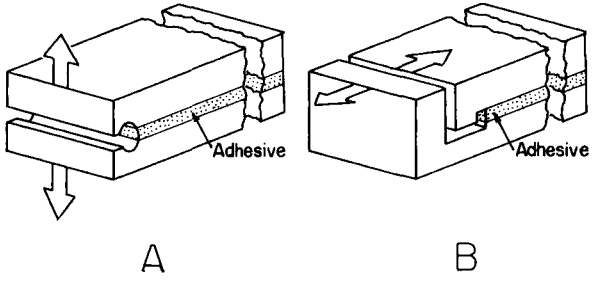

Figure 1. Test specimen configurations used by Ripling et. al. [6, 7, 9]. a. Test specimen for G_{IIc} measurement. b. Test specimen for G_{Ic} measurement.

The method described in this paper provides a measure of the fracture toughness of an adhesive-bonded joint in the lap-shear configuration. The description of the fracture toughness test method and results is followed by a discussion of the interpretation of the test results in terms of the standard modes of crack extension.

II. THEORY

A tensile load will pull both ends of a lap-shear sample into line with attendant bending of all parts as illustrated in Fig. 2. Each of the two interfaces is terminated at a "loading edge" where the load is transmitted from the adherend to the adhesive and at a "free edge" at the opposite end of the over-lap on that same interface. These are identified in Fig. 3. Interfacial separation begins at the loading edges, where the tearing stress is a maximum [10], and progresses towards the center of the joint.

Figure 4 schematically illustrates the structural features of a metal-adhesive interface. The metal is polycrystalline with a regular arrangement of atoms and is covered with an oxide, which is thin, firmly attached, and provides the sites for attachment of the adhesive molecules. The adhesive is made up of random branched and cross-linked molecular chain segments.

All of the structural micro-elements deform under load. These include atom-to-atom linkages in the metal (A-B), linkages between equivalent groups in the oxide (C-D), and free molecular segments in the polymer.

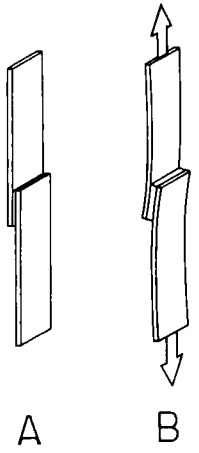

Figure 2. Lap-shear joint configuration. a. Undeformed. b. Under load.

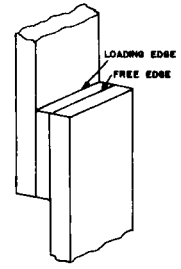

Figure 3. Features of the lap-shear joint. The loading edge and the free edge are indicated on the two interfaces at the same end of the overlap.

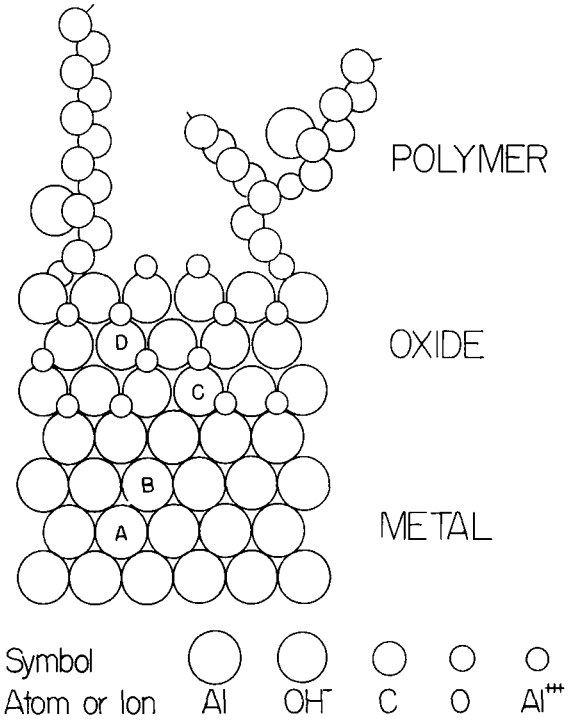

Figure 4. Structure (schematic) of phases in a metal-coherent oxide-polymer composite. The metallic phase is represented by a close packed plane of aluminum, the oxide phase is represented as Bayerite, $Al_2O_3 \cdot 3H_2O$, and the polymer is represented by aliphatic chain segments with reacted epoxide groups at the oxide surface. Hydrogens are not represented in any way. A and B are nearest metal neighbors and C and D are equivalent molecular groups in the oxide. A-B, C-D, and molecular chain segments between branches and other points of attachment are the load carrying structural elements.

Each may be extended or shortened by the distortion of primary bonds, the molecular segments may deform by rotations about carbon-carbon bonds, and individual elements may be sheared or rotated relative to neighboring elements.

When separation is nucleated it will progress as described above. Possible failure mechanisms include detachment at the surface, intramolecular scission, or withdrawal by inter-molecular slip. The first two involve elastic extension and the last is by shear.

The precise definition of the failure micro-locus is desirable but not essential for a measurement. Fracture mechanics is a macro-science in that it applies to materials rather than individual linkages. However, the applica-

tion of the results to adhesion studies requires this information. A change in observed fracture toughness may be due either to a change in properties or to a change in fracture micro-locus or mechanism.

The Irwin and Kies method of fracture toughness determination is based on the change of sample stiffness with crack area [3,8,11]. The stress field analysis method is not applicable due to the complexities inherent in the lap-shear sample configuration. Before deriving the equation, it will be shown that the work to extend a crack by a unit area, which is the measure of fracture toughness, is equivalent to the strain energy released by the sample. The effect of flow will also be explained. Finally the strain energy release rate, G, will be calculated for a lap-shear sample as shown in Figs. 2 and 3, but with identical cracks at each loading edge. Figure 5 shows the three step loading cycle that will be followed.

The first step is to directly increase the load to P_f. The sample extension over the gauge length is l_f and W_1 is the work performed on the sample in this deformation and is stored as elastic energy. This is shown in Fig. 6a.

$$W_1 = \tfrac{1}{2}P_f l_f \qquad (1)$$

The phenomenological relation describing the mechanical behavior of this sample is:

$$P = Ml \qquad (2)$$

M is the sample stiffness which depends upon the numbers and kinds of structural elements in the system. The applied load is P and l is the elongation. If the number of different kinds of structural elements is constant and

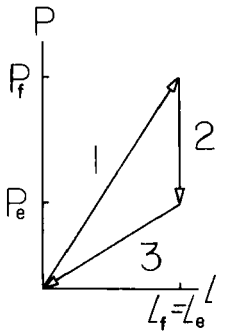

Figure 5. Loading cycle.

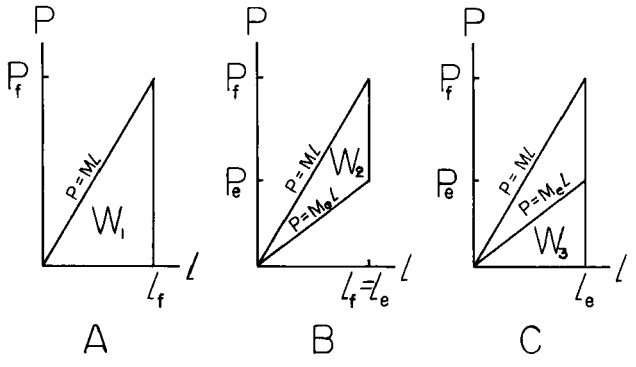

Figure 6. Elastic crack extension and associated work.

if each has a linear deformation characteristic the overall sample deformation characteristic will be linear as described by M. If either the number of elements or the proportions of the different elements should change, the value of M will change. If the applied load is released the sample will recover its original dimensions as will each deformation elements.

Crack extension (branch 2 of Fig. 5) is conducted starting at the load level, P_f. For this process the dimensions of the sample are controlled so that the gauge length extension, l_f, does not change. This "fixed grip" crack extension process is to be conducted in such a way that the relaxations of the remaining structural elements is elastic. Each element relaxation represents a small release of stored elastic strain energy. The sum is equal to the work, W_2, shown in Fig. 6b.

This change affects the parameters in equation (2). The load level drops from P_f to P_e. There is no change of extension, thus $l_f = l_e$. The sample stiffness decreases from M to M_e due to the reduction in number of structural elements. The process of elastic crack extension is defined as the progressive disconnection of structural elements at the crack edge.

The third step in this loading cycle is represented as branch 3 of Fig. 5. All strain, both macro- and microscopic, is recovered. In other words each element is relaxed. The elastic readjustments of the remaining elements are such that the final extension of each is proportional to its load, which is proportional to the load applied to the sample. The work, W_3, is recovered, stored elastic energy, shown in Fig. 6c.

Through the whole cycle the unrecovered work, W_1-W_3, is the strain energy released. Thus the work of crack extension is equivalent to the strain energy released.

$$W_2 = W_1 - W_3 \tag{3}$$

This could have been developed for fixed load conditions. The equivalence is explained by Irwin [8].

It should be noted that the sample stress relaxation in step 2, might have been accomplished by processes involving flow, which is the shift of structural elements to new equilibrium positions. These changes in connectivity are different from the process of disconnecting structural elements. In the crack extension process there is no inherent need for these shifts. They only provide an accommodation. Whether they occur at the crack edge or in any other location within the gauge length, the same results will be observed. The most significant aspect is that the numbers and kinds of structural elements are not greatly changed. Thus, the sample stiffness, M, is not changed. When the remaining applied load, P_e, is removed, the macro-relaxation is less than the original macro-elongation and a permanent set and internal stresses are left. See Fig. 7a.

Table 1. Fracture Toughness Sample Dimensions (Inches)

width b	overlap length	adherend thickness	adhesive thickness	sample length
½	1½	.065	.006	10

The adherends were made of aluminum alloy, Alclad 2024-T3, and the adhesive was a two part epoxy, EPON 934 (Shell Chemical Company). After machining, the adherends were degreased in acetone, and the portion to be bonded was dipped into a dichromate etching solution (2.85 gms. $K_2Cr_2O_7$, 28.5 gms. H_2SO_4, distilled water to make 100 ml.) for 12 minutes at a temperature in the range of 60-70°C. The adherends were than rinsed in cold tap water and dried by hot air. Nail polish was applied to mask the areas at the loading edges for the formation of the artificial cracks. A number of alternate methods were tried, but this produced the best results in terms of crack area definition and control.

The ASTM Special Committee on Fracture Toughness Testing investigated the effect of the radius of the crack tip on fracture toughness measurement [2]. They found that the effect was variable but that a radius of less than .001 inches would assure good "natural" crack simulation. The tip radius of the artificial cracks made with nail polish was between .0003 and .0004 inches and, therefore, should be similar in effect to natural cracks. The radius was determined by measuring the thickness of the nail polish as the crack tip diameter. As explained above, the absence of permanent deformation processes is the criterion for validity. This is confirmed by linearity in the load-elongation autographic chart record.

The adhesive was applied to the surfaces to be bonded and eight pairs of bonded adherends were placed into a clamping fixture that provided alignment and spacing as well as a spring-loaded device to maintain a force of approximately 20 pounds across the joints, in series. The curing cycle was 300°F for 30 minutes in air. After cooling and unclamping, the samples were ready for testing.

For fracture toughness testing, it is advantageous to use testing equipment that is stiff relative to the specimen. If too much elastic energy is stored in a relatively compliant machine, it is not possible to control crack extension.

A Tinius-Olsen universal testing machine of 300,000 pound capacity was used. This machine also includes a system for autographic recording of the load-elongation curve by means of a pneumatic load cell and a clamp-on LVDT extensometer. The gauge length of the extensometer is 2 inches,

E is the energy stored in the sample due to the work of elastic deformation. After differentiating and dropping the terms involving dl/dA, due to the fixed-grip conditions, equations (5) and (6) are obtained.

$$\frac{dP}{dA} = -MP\frac{d(1/M)}{dA} \tag{5}$$

$$\frac{dE}{dA} = -\tfrac{1}{2}l\frac{dP}{dA} \tag{6}$$

The strain energy release rate, G, is the elastic energy change, dE, due to the change in crack area, dA, and can be found by substituting (2) and (5) into (6). The result is:

$$G = \tfrac{1}{2}P^2\frac{d(1/M)}{dA} \tag{7}$$

This leads to the following expression for the strain energy release rate,

$$G = \frac{P^2}{4b}\frac{dC}{da} \tag{8}$$

at a load level, P, for a lap-shear joint of width, b, and identical cracks of length a, extending over the full sample width. The sample compliance, C, is the reciprocal of the sample stiffness, M.

Equation 9 expresses the conditions at the critical load level, P_c, when the crack extends rapidly, without flow.

$$G_c = \frac{P_c^2}{4b}\frac{dC}{da} \tag{9}$$

The result is the pair of equations that express the strain energy release rate for any level of loading and the critical strain energy release rate at which rapid elastic crack extension occurs for the lap-shear sample with two identical, rectangular cracks.

III. SAMPLES AND EXPERIMENTAL PROCEDURE

The specimens used for fracture toughness testing are in the lap-shear configuration, following the recommendations in standard test procedures [12]. The samples were assembled separately in batches of eight, rather than in panels, and the overall shape was a "dog bone" with a ¾ inch diameter hole in the large section at each end to allow pin mounting. Table 1 lists the sample dimensions, neglecting crack size, which was varied.

Table 1. Fracture Toughness Sample Dimensions (Inches)

width b	overlap length	adherend thickness	adhesive thickness	sample length
½	1½	.065	.006	10

The adherends were made of aluminum alloy, Alclad 2024-T3, and the adhesive was a two part epoxy, EPON 934 (Shell Chemical Company). After machining, the adherends were degreased in acetone, and the portion to be bonded was dipped into a dichromate etching solution (2.85 gms. $K_2Cr_2O_7$, 28.5 gms. H_2SO_4, distilled water to make 100 ml.) for 12 minutes at a temperature in the range of 60-70°C. The adherends were than rinsed in cold tap water and dried by hot air. Nail polish was applied to mask the areas at the loading edges for the formation of the artificial cracks. A number of alternate methods were tried, but this produced the best results in terms of crack area definition and control.

The ASTM Special Committee on Fracture Toughness Testing investigated the effect of the radius of the crack tip on fracture toughness measurement [2]. They found that the effect was variable but that a radius of less than .001 inches would assure good "natural" crack simulation. The tip radius of the artificial cracks made with nail polish was between .0003 and .0004 inches and, therefore, should be similar in effect to natural cracks. The radius was determined by measuring the thickness of the nail polish as the crack tip diameter. As explained above, the absence of permanent deformation processes is the criterion for validity. This is confirmed by linearity in the load-elongation autographic chart record.

The adhesive was applied to the surfaces to be bonded and eight pairs of bonded adherends were placed into a clamping fixture that provided alignment and spacing as well as a spring-loaded device to maintain a force of approximately 20 pounds across the joints, in series. The curing cycle was 300°F for 30 minutes in air. After cooling and unclamping, the samples were ready for testing.

For fracture toughness testing, it is advantageous to use testing equipment that is stiff relative to the specimen. If too much elastic energy is stored in a relatively compliant machine, it is not possible to control crack extension.

A Tinius-Olsen universal testing machine of 300,000 pound capacity was used. This machine also includes a system for autographic recording of the load-elongation curve by means of a pneumatic load cell and a clamp-on LVDT extensometer. The gauge length of the extensometer is 2 inches,

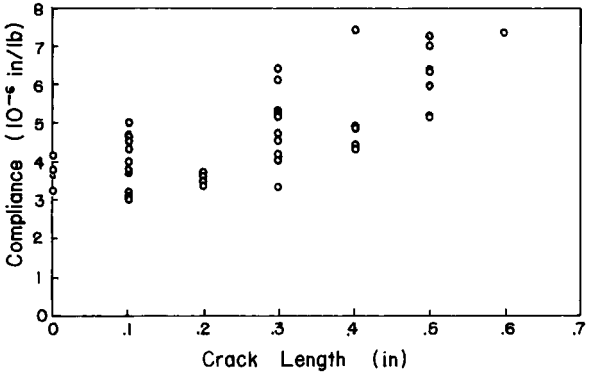

Figure 8. Compliance versus crack length, including all samples.

therefore the overlap of the samples was chosen to be slightly less to include the full overlap in the data and to allow a range of crack lengths. The cracks were varied in length from zero to .6 inches in increments of .1 inches. The uncracked, or ligament lengths varied from 1.5 to .3 inches.

The chart records, for the individual samples, provide information regarding the sample modulus, the critical load for rapid crack extension, and a direct evaluation of linearity to confirm the absence of permanent deformation in the measurement of compliance.

IV. RESULTS

An experimental program was planned to obtain values for the quantities required by equation (9). A number of specimens were tested for each of the crack lengths, as described above. The results are shown in Fig. 8. These results show only a weak correlation between compliance and crack length. Examination of the specimen fracture surfaces showed that a number had not bonded properly. The separation was predominantly along one interface only, the appearance of the epoxy surface was different, and permanent set in the adherends was less than in the others in which the separation developed symmetrically along the two interfaces from the loading edges with final tearing across the center of the overlap. The poorly bonded samples are more compliant, as is consistent with the smaller number of structural elements supporting the load at the interface. Fig. 9 shows the data for the well bonded samples. This shows a very definite trend.

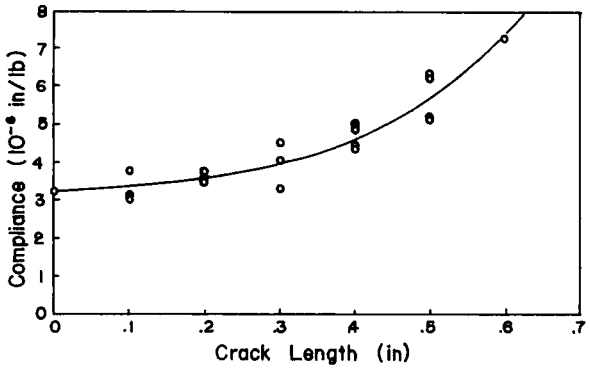

Figure 9. Compliance versus crack length after elimination of the data from poorly bonded samples and the curve of average compliance for each crack length versus crack length.

To calculate an equation of compliance as a function of crack length, the average value of compliance was found for each crack length. These values are also shown in Fig. 9. Using a computer least squares curve fitting program, an equation for the curve was obtained. The equation is:

$$C = 3.22 \times 10^{-6} + 8.13 \times 10^{-7}\, a + 1.38 \times 10^{-5} a^2 - 7.97 \times 10^{-5} a^3 + 2.08 \times 10^{-4} a^4 - 1.44 \times 10^{-4} a^5 \quad (10)$$

A polynomial expansion was used because no theoretical analysis was available to indicate what form of equation should be expected, and differentiation is direct. It was found that a fifth order polynominal yielded values to within three significant figures and was therefore, used. Table 2 compares the average experimental values of compliance with the computor calculated values.

Differentiating equation (10) with respect to a gives the following result:

$$\frac{dC}{da} = 8.13 \times 10^{-7} + 2.76 \times 10^{-5}\, a - 2.39 \times 10^{-4} a^2 + 8.24 \times 10^{-4} a^3 - 7.20 \times 10^{-4} a^4. \quad (11)$$

Substituting equation (11) into equation (9), yields the expression for the critical strain energy release rate, G_c, in polynomial form.

$$G_c = \frac{P_c}{b} (2.03 \times 10^{-7} + 6.90 \times 10^{-6} a - 5.98 \times 10^{-5} a^2 + 2.06 \times 10^{-4} a^3 - 1.80 \times 10^{-4} a^4). \quad (12)$$

To obtain G_c, the value of breaking strength, P_c, corresponding to a particular crack length, a, was obtained from the data. Table 3 lists the results of the calculations.

Ripling, et. al. found that G_c ranged from 1 to 2 in.-lb./in.^{2} for their samples in the configuration shown in Fig. 1a [9]. The results of these two determinations show very good agreement and support the validity of the use of samples in the lap-shear configuration. The narrow range of values, the ease in sample preparation, the rapidity of testing, and the possibility of using standard test equipment are features that favor the use of fracture toughness testing to study adhesion.

V. DISCUSSION CONCERNING THE MODE OF CRACK EXTENSION

The stress field at the crack edge determines the mode of crack extension

Table 2. Comparison of Experimental C and Computor C

a (in.)	*Experimental C* (in.lbs/in.^{2})	*Computer C* (in.lbs/in.^{2})
0.000	0.322×10^{-5}	0.3220×10^{-5}
0.100	0.338×10^{-5}	0.3379×10^{-5}
0.200	0.358×10^{-5}	0.3583×10^{-5}
0.300	0.389×10^{-5}	0.3887×10^{-5}
0.400	0.450×10^{-5}	0.4502×10^{-5}
0.500	0.562×10^{-5}	0.5619×10^{-5}
0.600	0.724×10^{-5}	0.7240×10^{-5}

Table 3. Breaking Load and Fracture Toughness Versus Crack Length

a (in.)	P_c (lb.)	G_c (in.lbs/in.^{2})
.1	1200	1.39
.2	1110	1.35
.3	844	1.42
.4	584	1.35
.5	425	1.18

Average $G_c = 1.39$

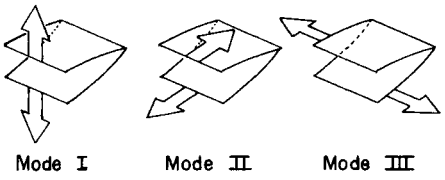

Figure 10. Crack extension modes. The drawings represent the forces acting on the crack surfaces.

[13, 14]. The three basic modes are shown in Fig. 10. Mode I, crack extension is caused by tearing stresses acting on the surfaces of the crack. Shear stresses on the surfaces of the crack, perpendicular or parallel to the crack edges, result in Mode II or Mode III crack extension, respectively. The measured fracture toughness is usually identified with the mode of crack extension by the appropriate Roman Numeral subscript, e.g. G_{Ic} which is the critical strain energy release rate in the opening mode.

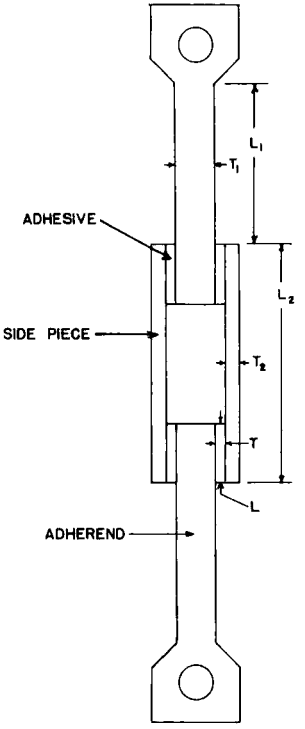

Figure 11. Dimensions of the photoelastic models in the symmetrical double lap configuration. See Table 4 for specific values for each dimension.

The mode of crack extension in a lap-shear joint is obscured by the complexity of the deformation. The authors feel, however, that there is sufficient evidence to identify the crack extension process in the lap-shear sample with the opening mode. This evidence is presented for consideration, although it is derived from samples in a different, but similar, configuration. It is felt that this conclusion will bear the test of time and experience because the correspondence in sample configurations is strong.

The argument is based upon the nature of the stress field in the adhesive-bonded joint, initially and in the presence of the crack. The evidence was obtained by using transparent photoelastic models in the symmetrical double lap configuration [15, 16]. This configuration involves four metal-adhesive interfaces, as shown in Fig. 11. Each has a loading edge and a stress field that is similar to that of a lap-shear interface as a result of a similar displacement in the load line in each [10]. The major differences between the stress distributions at the interfaces in the two configurations occur toward the free edge. Cracks nucleate and spread from the loading edges in both.

The sample dimensions in Table 4 refer to Fig. 11. The results from only

Table 4. Dimensions and Materials Used in the Photoelastic Models in the Symmetrical Double-Lap Configuration. Refer to Figure 11.

A. Dimensions (inches)

Model	Adhesive		Adherend		Side Piece	
	L	t	L_1	t_1	L_2	t_2
B	3	¼	2	¾	9	¾
C_2	2	¼	2½	1	6	1

B. Materials

Material	Young's Modulus (10^5 psi)	Source
Hysol-4439	4.75	Commercial Plastics and Supply Company, Atlanta, Georgia.
CR-39	2.5	Commercial Plastics and Supply Company, Atlanta, Georgia.
Duro Plastic Epoxy	—	Woodhill Chemical Company, Cleveland, Ohio.

two samples are reported, they are typical of a number of others that were studied. Model B is monolithic. It was cut from a sheet of Hysol-4439. In model C2 the adherends and side pieces were made of Hysol-4439 and the adhesive was represented by pieces of CR-39. Pieces of the two photoelastic materials were cemented together with thin layers of Duro plastic epoxy which was found to have a negligible effect on the stress patterns. This was shown by comparing the fringe patterns of a monolithic sample of Hysol-4439 in the above shape with a multilithic photoelastic sample in the same shape formed by gluing cut pieces of Hysol-4439. The samples are ¼ inches thick.

Fig. 12 shows the distribution of tearing and shear stresses along an interface from the free edge to the loading edge. These curves were plotted from the photoelastic stress patterns on model C2. These stress patterns are typical of many for samples with a variety of materials and dimensions. The features of the curves are that the maximum tearing stress occurs at the loading edge and that the interfacial shear stress is zero at the loading edge and reaches its maximum further along the overlap. Fig. 13 shows the original and deformed (under load) shapes of one interface with the deformation exaggerated relative to the sample dimensions.

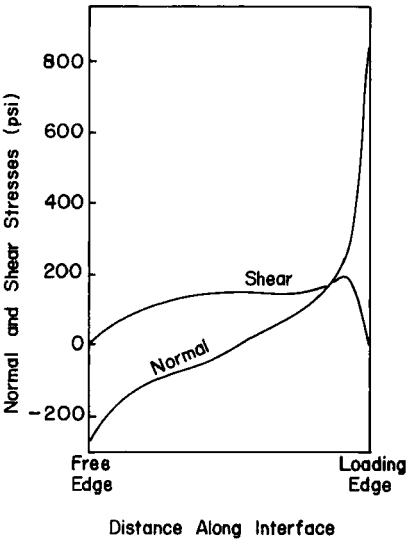

Figure 12. Normal stress (tearing stress) and shear stress along the interface of model C2.

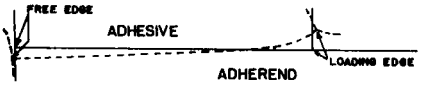

Figure 13. Approximate shape of model C2 before loading (solid line) and as deformed under load (dashed line).

Figure 14 shows the isochromatic and isoclinic patterns about one of the interfaces in sample B. The isochromatic pattern represents the loci of maximum normal stress of various levels of intensity. The isoclinic pattern shows the presence of isotropic points where isoclinic lines of all inclinations pass. There is an isotropic point at each loading edge. Other isotropic points occur in the samples, but do not directly affect the analysis. Each isotropic point is a point of no shear stress. Figure 15 shows the patterns of isoclinics after saw cuts were made at the two loading edges at one end of the bonded section. These were made to simulate cracks that grew along the interface from the loading edge [17]. Determinations were made with one quarter and one-half inch long cuts. The patterns may be compared with the isoclinic pattern in Fig. 14b for the same sample without cuts. This result, too, is typical of the results of a number of similar determinations.

The isotropic point moves along with the edge of the crack; shear stresses never act at the edge of the crack. The significance is that only tearing stresses act on the loading edge of the sample or on the crack edge as it moves. It is therefore believed that the lap-shear sample directly provides the same deformation mode and mechanism as the Ripling opening mode sample shown in Fig. 1a.

ACKNOWLEDGMENTS

The research was partially supported by Research Project No. DA-01-021-AMC-12832(Z) and by the Engineering Experiment Station at Auburn University. The authors acknowledge the assistance of Professor W. F. Swinson, Auburn University and Messrs. E. J. Wheelahan and E. A. Verchot, Army Missile Command, Redstone Arsenal, Alabama.

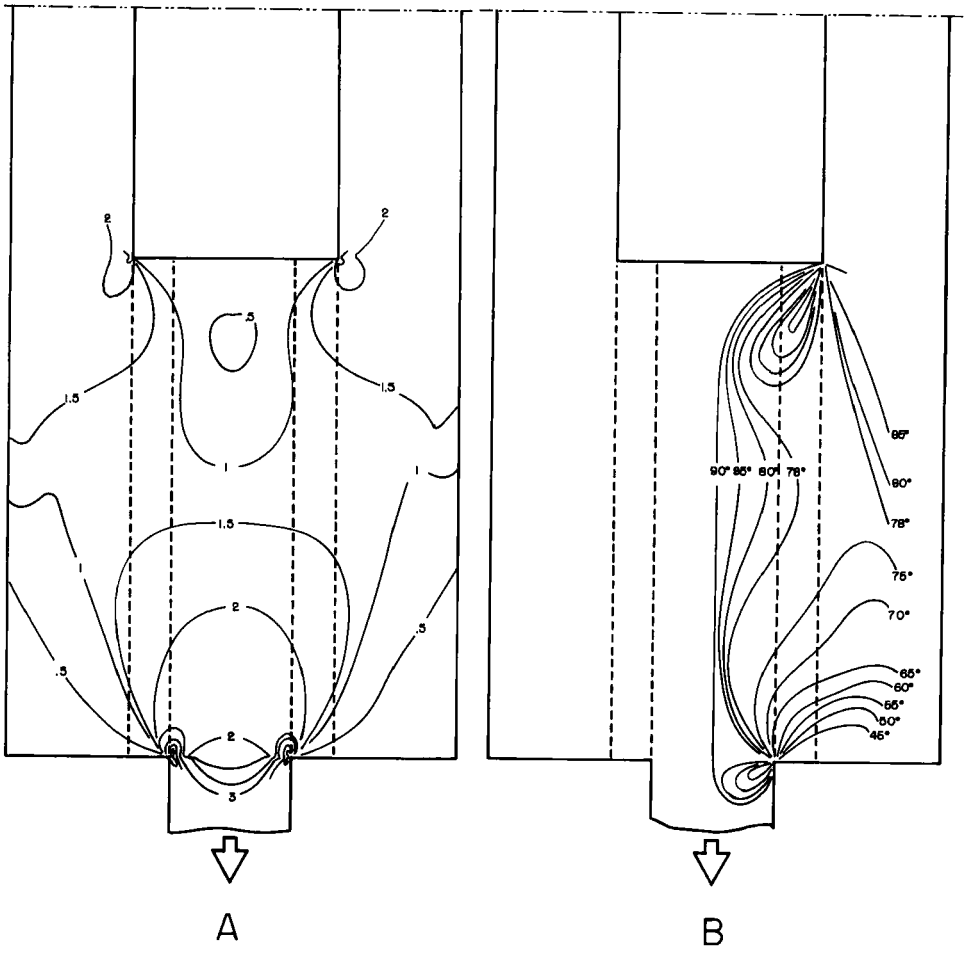

Figure 14. Photoelastic stress patterns on model B. a. Isochromatics. b. Isoclinics.

NOMENCLATURE

a	crack length
A	crack area
b	crack and sample width
C	sample compliance
E	deformation energy
G, G_c	strain energy release rate and its critical value
G_I, G_{Ic}	strain energy release rate in the opening mode and its critical value
l, l_e, l_f	gauge length extensions
L, L_1, L_2	lengths
M, M_e	sample stiffness

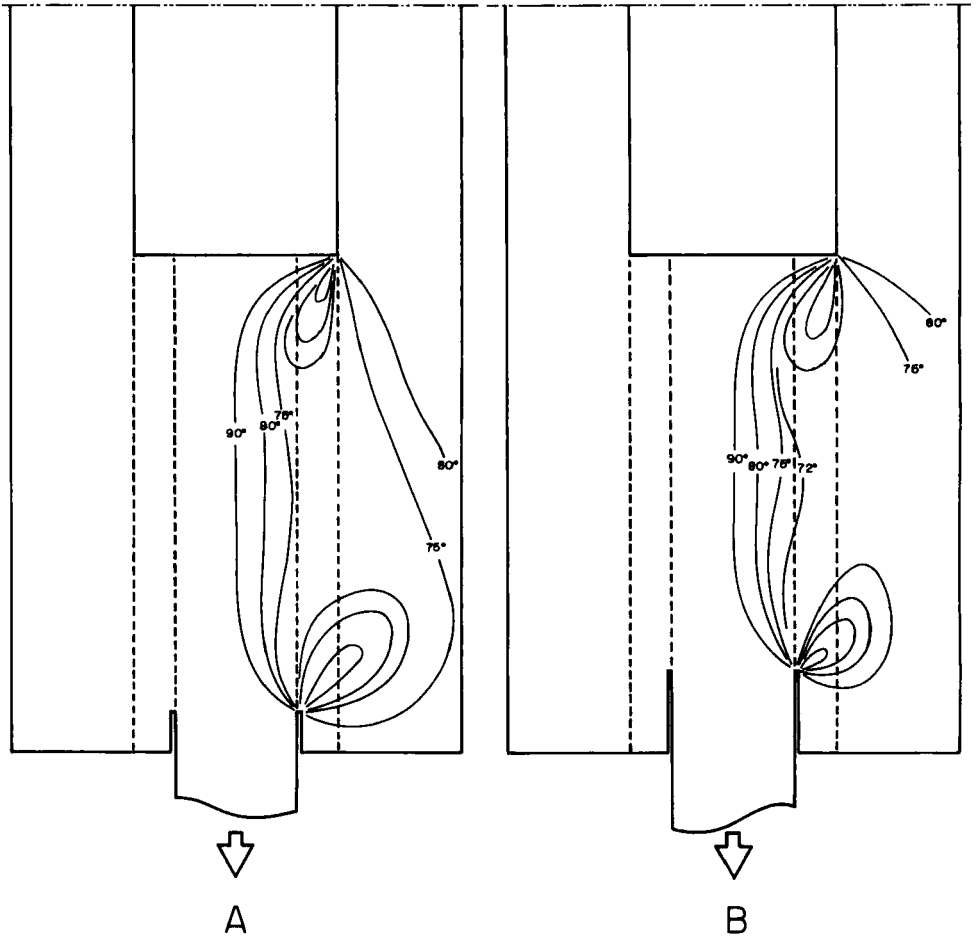

Figure 15. Isoclinic patterns near the interface in model B with cuts. a. Simulated crack length of one quarter inch. b. Simulated crack length of one half inch.

P, P_c	load and its critical value
t, t_1, t_2	thicknesses
W_1, W_2, W_3, W_4, W_5	work of deformation

REFERENCES

1. A. A. Griffith, "The Phenomena of Rupture and Flow in Solids," *Phil. Trans.*, Roy. Soc. (London), Series A, Vol. 221 (1920) pp. 163-198.
2. First Report of the Special ASTM Committee, "Fracture Testing of High-Strength Sheet Materials," ASTM *Bulletin*, No. 243, (1960) pp. 29-40.
3. G. R. Irwin, "Fracture Mechanics," *Structural Mechanics*, ed. by J. N. Goodier and N. J. Hoff, Pergamon Press, (1960) pp. 557-594.

4. G. R. Irwin, "Fracture Dynamics," *Fracturing of Metals,* ASM, (1948), pp. 147-166.
5. J. L. Gardon, "Variables and Interpretation of Some Destructive Cohesion and Adhesion Tests," *Treatise on Adhesion and Adhesives,* Vol. I, ed. by R. L. Patrick, Marcel Dekker Inc., (1967), pp. 269-324.
6. E. J. Ripling, S. Mostovoy, and R. L. Patrick, "Measuring Fracture Toughness of Adhesive Joints," *Mats. Res. and Stds.,* Vol. 4, (1964), pp. 129-134.
7. E. J. Ripling S. Mostovoy, and R. L. Patrick, "Application of Fracture Mechanics to Adhesive Joints," *Adhesion,* STP 360, ASTM (1964).
8. G. R. Irwin, "Fracture Mechanics Applied to Adhesive Systems," *Treatise on Adhesion and Adhesives,* Vol. I, ed. by R. L. Patrick, Marcel Dekker, Inc., (1967), pp. 233-268.
9. S. Mostovoy and E. J. Ripling, "Factors Controlling the Strength of Composite Bodies," Final Report, Contract NOW 64-0414-c, (1967)
10. K. Masubuchi and R. E. Keith, "Fundamentals of Deformation Characteristics of Adhesive-Bonded Joints and Metal-Adhesive Interfaces," Final Report, Contract No. DA-01-021-AMC 14693(Z), (1967).
11. G. R. Irwin and J. A. Kies, "Critical Energy Rate Analysis of Fracture Strength," *Welding Journal* (Research Supplement), Vol. 33, (1954), pp. 193s-198s.
12. ASTM Method D 1002.
13. P. C. Paris and G. C. Sih, "Stress Analysis of Cracks," *Fracture Toughness Testing and Its Applications,* STP 381, ASTM, (1964), pp. 30-81.
14. W. F. Brown, Jr. and J. E. Srawley, *Plane Strain Crack Toughness Testing of High Strength Metallic Materials,* STP 410, ASTM, (1966), pp. 1-65.
15. R. K. Diwan, "A Photoelastic Technique for the Determination of Stresses Across the Interface of Metal-to-Metal Bonded Double Lap Joint," Thesis submitted in partial fulfillment of the requirements for the Master of Science Degree, Auburn University, (1967).
16. W. A. Jemian, "Study of the Onset of Permanent Deformation in Structurally Bonded Joints," Quarterly Report No. 8, Contract No. DA-01-021-AMC(12832)Z, (1967), pp. 2-12.
17. J. F. Phillips, "The Effect of a Tear on an Isotropic Point in a Bonded Joint," Senior Thesis, Auburn University, (1968).